JCTC Journal of Chemical Theory and Computation

Article

pubs.acs.org/JCTC

Short Time Dynamics of Ionic Liquids in AIMD-Based Power Spectra

Katharina Wendler,[†] Martin Brehm,[‡] Friedrich Malberg,[‡] Barbara Kirchner,[‡] and Luigi Delle Site*[,§]

[†]Max-Planck-Institut für Polymerforschung, Ackermannweg 10, D-55128 Mainz, Germany

[‡]Universität Leipzig, Linnéstraße 2, D-04103 Leipzig, Germany

[§]Institute for Mathematics, Freie Universität Berlin, Arnimallee 6, D-14195 Berlin, Germany

Supporting Information

ABSTRACT: Power spectra of several imidazolium-based ionic liquids, 1,3-dimethylimidazolium chloride, 1-ethyl-3-methylimidazolium thiocyanate, 1-ethyl-3-methylimidazolium dicyanamide 5, 1-butyl-3-methylimidazolium chloride, 1-butyl-3-methylimidazolium thiocyanate, and 1-butyl-3-methylimidazolium dicyanamide, are presented based on ab initio molecular dynamics simulations. They provide an alternative tool of analysis of several electronic structure-based properties, in particular, those related to the strength of hydrogen bonding in liquids. Moreover, they can be employed to interpret experimental IR or Raman spectra, avoiding the additional calculations required for theoretical IR or Raman spectra. The obtained power spectra are shown to be in good agreement with experimental spectra, and electronic structure properties related to them are analyzed. Further, there are indications for a locality of the power spectra on a relatively short time scale of ≈10 ps or system size of about 8 ion pairs as already speculated in previous work.

1. INTRODUCTION

During the last years, ionic liquids (ILs) were established as a new promising class of substances. However, theoretical predictions have not proceeded parallel to the large experimental activity,[1−10] and the fundamental understanding of the molecular origin of macroscopic properties still lacks a solid theoretical predictive basis.[11] ILs are indeed a real challenge for theoreticians due to their high complexity. They show structural and dynamical heterogeneity as their properties are determined on a molecular scale by the subtle balance between Coulomb[12−15] and van der Waals forces[12,16−19] as well as hydrogen bonding[18−28] and entropy.[29] As a consequence, the prediction of ILs' properties is rather difficult in general. Due to the high number of possible ion combinations forming, potentially, millions of different ILs, a solid tool is highly required for the rational design of systems with properties on demand. Thus, theoretical models for designing systems in silico are needed. In the development of such models, the validation by experimental data is crucial in order to ensure reliability.

That is why this paper is focused on the properties linked to the short time dynamics of ILs, such as hydrogen bonding or ion pair formation, which are well within the time scale of IR or Raman spectra.[21,30−38] These spectra are very helpful in order to evaluate the electronic structure and possible reactions in mixtures[30] and to study hydrogen bonds[21,31,33,35−37,39] or rotational isomerism of the butyl chain[33] as well as preferred anion conformations.[34,40] For instance, the influence of hydrogen bonding on large scale properties, which is a widely discussed topic in IL research, was elucidated by elaborated IR studies.[21,35,36,39] However, the experimental spectra describe the sum of all present vibrations and rotations, and the assignment of signals to specific vibrations requires additional analysis. There, theoretical atomistic studies allow for a complemental insight.

In this perspective, molecular dynamics (MD) simulations would be a powerful tool if the corresponding force fields are trustworthy. The comparison between IR or Raman spectra from experiments and those derived from theoretical calculations would be an elegant way to evaluate the reliability of the theoretical results on molecular length and time scales. Such a comparison can be employed to check if a model is likely to describe the correct molecular mechanisms or not. In general, limitations of theoretical models, such as, e.g., inaccurate description of some specific interactions, may lead to changed frequencies of the connected vibrations in the spectra. These deficiencies in the vibrational spectra of theoretical models could be used to understand where the molecular description fails and, thus, to improve the model. For instance, it was found that the underestimation of the hydrogen-bond strength gave too high viscosities in classical MD simulations.[24,41] In addition, a general time shift might occur due to approximations present in any model. One should consider to apply this shift also to, e.g., theoretically predicted life times of conformations. Ab initio results, often used as reference for classical models[42] and, thus, to build new models, might be subject to such a general time shift which is tested in this work.

On the basis of a well-founded force field, MD studies allow for the determination of the molecular origin of a signal in a direct way as theoretical spectra can be calculated for specific parts of the whole system, such as certain atom groups or single molecules in special conformations. This information can be combined with data about, e.g., life times of certain conformations and a more detailed understanding of the interplay between the different aspects would naturally emerge. Beyond classical MD, ab initio MD (AIMD) simulations

Received: February 21, 2012
Published: April 4, 2012

ACS Publications © 2012 American Chemical Society

describe the fluctuations in the molecular electronic structures and can broaden the knowledge by the study of, e.g., electric dipole moments, polarization processes, or possible charge-transfer effects. AIMD-based spectra should reproduce the red shift of CH vibrations caused by hydrogen bonding. However, AIMD simulations are computationally demanding, and only relatively small systems of tenths of ion pairs can be propagated over short time periods of tenths of picoseconds.

Possibly, information on electronic effects could be gained in computationally less demanding ab initio studies of gas-phase ion pairs or even of the ground-state structures. In literature, the experimental spectra are often interpreted with the help of ab initio-based vibration frequencies of single ions or ion clusters in their ground state.[21,32−38,43−45] However, ground-state studies of small structures cannot describe the vibrational spectra typical for the liquid phase which are the result of the cooperativity of many molecules' interactions. The anharmonicity of the vibrations can be described by AIMD-based spectra at least in principle, but it is mostly neglected in the frequency analysis of ground-state structures. One possibility to lower the computational demand of AIMD-based spectra is to simulate smaller systems for shorter times. It has been shown that the molecular electrostatic properties of ILs were rather local and that simulations of liquid-like systems as small as eight ion pairs describe these properties with sufficient accuracy.[46,47] In this perspective, it will be important to test if a similar independence is found for AIMD-based spectra. This would be crucial for the potential of AIMD-based spectra as an unique and general tool to study the short time dynamics of ILs.

Due to the prohibitive computational costs, only few IR spectra have been calculated based on AIMD simulations in general[48−51] and none for an IL system. Even though it was shown that relatively short simulation times of 10 ps were sufficient to obtain an IR spectra reproducing the experimental one,[50,51] the evaluation of the selection rule is computationally demanding as it is also for Raman spectra. In general, IR and Raman spectra cover the same frequency range, but the selection rules are different and the observed signals vary. An alternative way to look at vibrational properties are the power spectra, which capture all present vibrational−rotational movements of the systems and not only the IR or Raman active ones. The wavenumbers and the origin of the signals are the same as the ones in the corresponding IR and Raman spectra, but the signal intensities do not have to be similar. In this way, power spectra can help to interpret the signals found in experimental spectra without predicting IR or Raman spectra.

Power spectra have the advantage that their calculation does not affect the computational cost of the AIMD simulation, as no selection rule has to be evaluated (see Section 2). Despite the low computational demand, power spectra were not considered in the numerous AIMD studies of ILs,[19,23,52−62] except in the works of Bhargava et al.[20,63] and Sarangi et al.[64] There, the power spectra of deuterated 1,3-dimethylimidazolium chloride[20] and a mixture of deuterated 1-ethyl-3-methylimidazolium chloride and hydrogen fluoride[63] were calculated to show the influence of hydrogen bonding on the C^2D bond vibration. Also, the influence of hydrogen bonding on the low wavenumber modes has been studied by classical simulations which were compared to AIMD simulations of crystalline 1-butyl-3-methylimidazolium hexafluorophosphate.[64] In general, the quality of the power spectra increases as the system size and the simulation time increase, like possible in classical MD simulations. But current classical MD approaches often constrain the CH bond lengths in order to allow for a larger time step or neglect the anharmonicity of the vibration. Hence, power spectra obtained on MD simulations are not meaningful at least for high wavenumbers at which the hydrogen vibrations occur. Power spectra based on AIMD simulations, despite possible limitations on the size and the time scale considered, may offer a unique tool in the study of the short time dynamics in ILs.

In the following, the potential of such power spectra is demonstrated for six different ILs, 1,3-dimethylimidazolium chloride (MMIM Cl), 1-ethyl-3-methylimidazolium thiocyanate (EMIM SCN), 1-ethyl-3-methylimidazolium dicyanamide (EMIM DCA), 1-butyl-3-methylimidazolium chloride (BMIM Cl), 1-butyl-3-methylimidazolium thiocyanate (BMIM SCN), and 1-butyl-3-methylimidazolium dicyanamide (BMIM DCA) (for nomenclature see Figure 1). After a short excursus on the calculation of power spectra in Section 2, the power spectra based on AIMD simulations are compared to experimental data in Section 4.1. A good agreement to the experimental spectra was found for AIMD data of liquid-like systems but not for systems of isolated ion pairs or ground-state structures, as discussed in Section 4.2. Further, the impact of hydrogen bonding was studied in Section 4.3, and it is shown how AIMD data can assist the interpretation of these signals and for those associated with the side chain of the imidazolium cations (see Section 4.4). In this way, this work illustrates the potential of AIMD-based power spectra as a new tool in the theoretical studies of ILs.

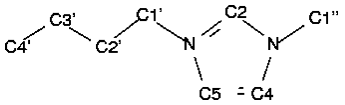

Figure 1. Nomenclature of the carbon atoms in imidazolium ions for the example of BMIM.

2. METHODOLOGY

The power spectrum (or power spectral density) is the Fourier transform $S(f)$ of the velocity autocorrelation function $R(\tau)$:[65]

$$S(f) = \int_{-\infty}^{\infty} R(\tau) e^{-2\pi i f \tau} d\tau \quad (1)$$

if assuming a wide-sense stationary random process and applying the Wiener−Khinchin theorem.[66,67] In order to obtain the power spectrum, the velocity autocorrelation function is calculated for each atom in the three directions x, y, and z. Due to the short simulation times, the autocorrelation is calculated, starting at all timesteps. Subsequently, the sum of all these autocorrelation functions is determined by

$$R(\tau) = \langle v(0) \cdot v(\tau) \rangle \quad (2)$$

$$= \frac{1}{3N(t_{end} - \tau)} \sum_{n=1}^{N} \sum_{i=1}^{3} \sum_{t=0}^{t_{end}-\tau} (v_{n,i}(t) \cdot v_{n,i}(t + \tau)) \quad (3)$$

in which N is the number of atoms, τ a time interval, t_{end} the timelength of the trajectory, $v_{n,i}$ the velocity component of atom n in direction i, and i sums over the three coordinates x, y, and z. Finally, the Fourier transform is calculated, and a Hanning window function[68] is applied as filter in the time domain in order to increase the quality of the spectra. The time domain

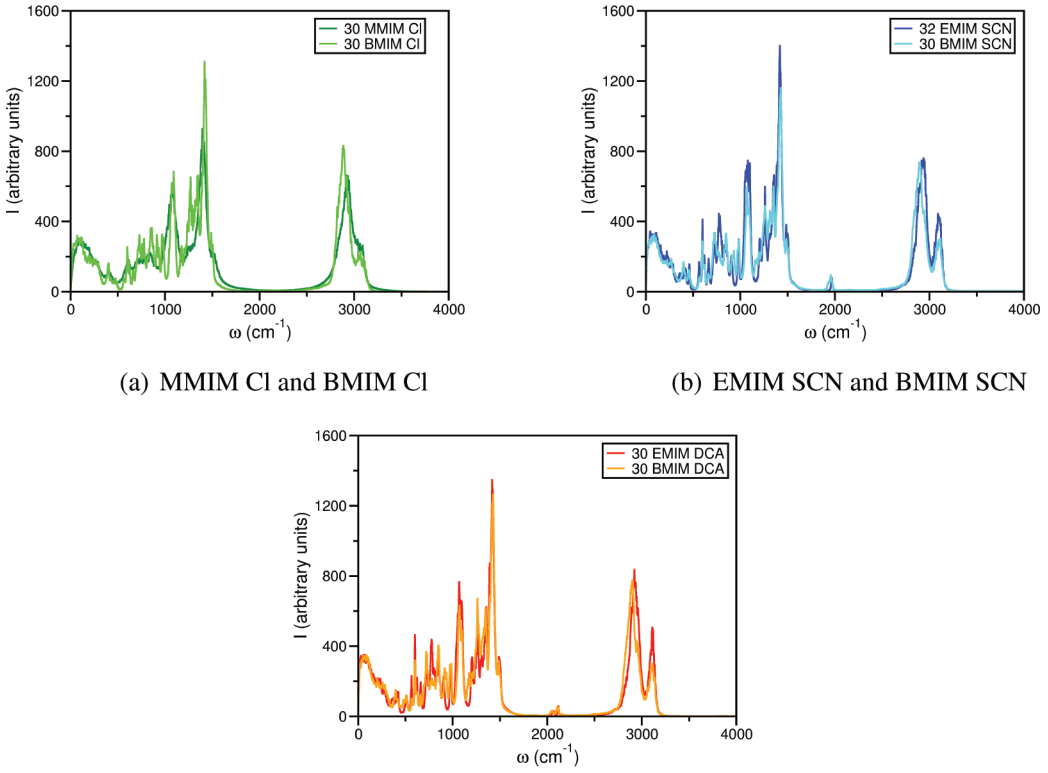

Figure 2. Power spectra of (a) MMIM Cl and BMIM Cl, (b) EMIM SCN and BMIM SCN, and (c) EMIM DCA and BMIM DCA.

signal is evenly symmetrized about the origin[68] ($R(\tau) = R(-\tau)$), and zero padding is applied. The power spectra can be calculated easily with a program, such as TRAVIS,[69] as was demonstrated for an AIMD system of 32 EMIM SCN ion pairs.[69]

The time scale τ might deviate from the real times which would lead to shifted frequencies. Indeed, such a time scale shift exists due to the present approximations in the quantum method, such as the truncated basis set, the functional and its approximation of the exchange-correlation, and, special in Car–Parrinello MD (CPMD), the fictitious electron mass. As a consequence, the obtained wavenumbers need to be corrected. In the present AIMD studies, both the fictitious mass of 400 au and the BLYP functional slow down the dynamics. A hypothetical fictitious electron mass of 450 au was proposed to include both effects.[50] Thus, the wavenumbers have to be corrected by $\omega_{corrected} = \omega(1 + (\delta M/M))^{1/2}$ [49] in which M is the sum over the nucleic masses of the vibrating atoms and δM is the sum over the fictitious masses of the associated electrons. Obviously, the masses M and δM depend on the atoms actually involved in a certain vibration. As a consequence, the wave function correction should be specific for each vibration. However, the assignment of the involved molecule parts is not a priori possible, and the corrections will have similar values. Thus, it is well established to choose a general correction factor.[50,51,70] For an imidazolium cation, the mass including the fictitious mass correction is about 1.100 times the value of the real mass, hence, the wavenumber correction factor is 1.049. Analogously, the wavenumber correction for DCA is a factor of 1.042, for SCN 1.030, and for Cl 1.024. As a universal correction factor was needed within this work, it was chosen arbitrarily to be 1.045, which gave results rather consistent with the experimental data (see Section 4.1). For water spectra in literature, higher correction factors of 1.115,[50] 1.117,[51] or 1.414[70] were proposed after fitting to the experimental data.

3. COMPUTATIONAL DETAILS

Car–Parrinello molecular dynamics[71] simulations were performed to study liquid-phase properties of several ILs by using the CPMD package.[72] In all simulations, the Kohn–Sham orbitals were expanded in a plane wave basis with a kinetic energy cutoff of 35 E_h (70 Ry), the fictitious electron mass was 400 m_e. Periodic boundary conditions, a time step of 0.1 fs (4 au) and standard Nose–Hoover thermostats[73,74] for atoms and electrons were applied. The BLYP functional[75,76] with Troullier–Martins pseudopotentials, derived using the BLYP functional, and an empirical dispersion correction[77] were employed unless otherwise specified. This setup has been recommended in literature.[78,79] Unless otherwise specified, the simulations were started from an equilibrated snapshot of a classical MD simulation,[42] and the equilibration time was chosen to be 5 ps. An overview of the systems is given below:

(1) 30 ion pairs MMIM Cl, 425 K, $(1.805\ nm)^3$, 25 ps, PBE functional (more details in ref 55)
(2) 30 ion pairs BMIM Cl, 400 K, $(2.021\ nm)^3$, 22.85 ps
(3) 32 ion pairs EMIM SCN, 400 K, $(2.006\ nm)^3$, 11.24 ps (started from an ab initio trajectory[23] snapshot, 0 ps equilibration, more details in ref 46)
(4) 30 ion pairs BMIM SCN, 400 K, $(2.134\ nm)^3$, 16.44 ps
(5) 1 ion pair EMIM DCA, 400 K, $(2.000\ nm)^3$, 77.6 ps
(6) 8 ion pairs EMIM DCA, 400 K, $(1.311\ nm)^3$, 63.50 ps (more details in ref 46)
(7) 30 ion pairs EMIM DCA, 400 K, $(2.037\ nm)^3$, 43.98 ps (more details in ref 46)

dx.doi.org/10.1021/ct300152t | J. Chem. Theory Comput. 2012, 8, 1570–1579

(8) 30 ion pairs BMIM DCA, 400 K, $(2.174\ nm)^3$, 15.48 ps

In the present work, the data of the recent simulations[46,55] were analyzed under the new aspect of power spectra in order to allow for a broader comparison. The power spectra, dihedral distributions, and spacial distribution functions were calculated with TRAVIS.[69]

4. RESULTS AND DISCUSSION

At a first glance, the spectra of imidazolium based ILs with longer and shorter side chains were rather similar (see Figure 2), and different anions did not change the spectra drastically (see Figure 2). The similarity of the spectra implied that reliable and consistent power spectra were obtained on data covering the dynamics of about 30 ion pairs and as few as 10 ps. The statistics in a short time intervals of 10 ps seemed sufficient for the determination of power spectra, which were in agreement with power spectra based on longer times of about 20 ps. Hence, typical AIMD simulations were found to be suitable for the power spectra study and prove that this may be a useful, computationally applicable tool indeed. However, power spectra based on AIMD simulations should be consistent not only with other AIMD based ones but also mainly with experimental spectra. This is shown in the next subsection.

4.1. Comparison to Experimental Spectra. In general, the corrected wavenumbers of the signals in the power spectra (as shown in Figure 2 and in the Supporting Information) were in good agreement to experimental IR and Raman spectra,[21,30−35,38,80] in contrast to the signal intensities. Hence, the method used here describes the dynamics in a reliable way after applying a correction factor of 1.045 which was a result of the known approximations of CPMD (see Section 2). A simulation time of 10 ps seemed sufficient to sample the short time dynamics observed by experimental spectra. This is a strong indication for the time locality of these processes. The ring CH bond stretch vibrations were reported to be between 3050 and 3200 cm^{-1} in BMIM Cl,[30,33,80] which was consistent with the range from 3040 to 3150 cm^{-1} found here (see Figures 2 and 6a). The same range was observed for other imidazolium-based ILs.[31−34,38,80] All signals in the power spectra could be matched to experimentally observed signals. However, there were some signals which were found in all experimental IR spectra but not in the power spectra calculated here. These were bands at about 1580 and 1170 cm^{-1} which were interpreted as imidazolium ring-bending modes.[32,38] The reason why these bands were missing in the power spectra is not yet understood; possibly, the dipole moment of these modes changes drastically, whereas the atoms move little. In general, the power spectra bands were rather broad and the resolution below that of experimental IR spectra. Currently, the short simulation times and the small system sizes do not allow for higher resolution.

The anion vibrations (see Figure 3) were found at wavenumbers similar to those of experimental IR spectra of reference substances. For the monatomic chloride, no other vibration was detected except the signal in the region around 100 cm^{-1}. For SCN, the three bands at 460, 730, and 1960 cm^{-1} were slightly below the experimentally observed signals of solid sodium thiocyanate at wavenumbers of 497, 755, and 2075 cm^{-1}.[81] Similarly, the signals of DCA were found at lower wavenumbers compared to solid sodium dicyanamide,[82] for instance 2110 cm^{-1} instead of 2230 cm^{-1} or 625 cm^{-1} instead of 664 cm^{-1}. Apart from these shifts, all signals of the DCA anion were present in the power spectra. The bending mode of the DCA anion was detected at about 160−170 cm^{-1} as in experiments.[21] The systematic underestimation of the vibration wavenumbers could be balanced by a larger correction factor. Yet, there might be some physical reason for the shifts, as the ions in ILs are governed by interactions present in the liquid phase but not in a salt crystal. In general, for anion power spectra, as given in Figure 3, there was a broad band around 100 cm^{-1} indicating that all anions took part in some intermolecular cation−anion vibrations[21] (see also Section 4.3). At this point, it can be concluded that power spectra based on AIMD simulations of the liquid phase were sufficiently consistent with the signals detected in experiments. However, the AIMD simulations of about 30 ion pairs considered here were computationally demanding. In the next section, the possible advantage of systems smaller than 30 ion pairs and their ablility to reproduce the same power spectra is discussed.

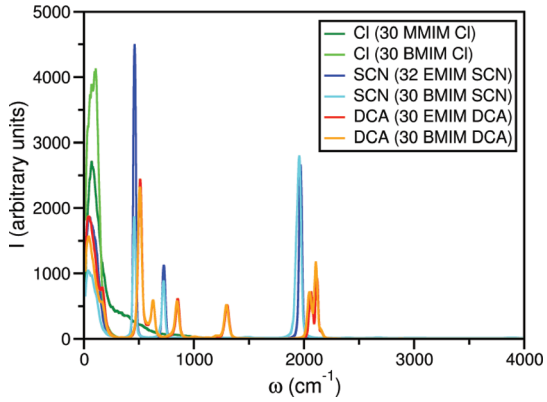

Figure 3. Part power spectra of the anions in all studied ILs.

4.2. Spectra of Different States. The IR frequencies of the ground state of small clusters or ion pairs have been studied intensively.[21,32−38,43−45] Due to the small number of atoms, high-level quantum chemical post Hartree−Fock methods can be applied next to density functional theory (DFT). However, the effect of temperature and entropy is completely missed, and this may influence the obtained spectra significantly. Instead, an isolated ion pair can be simulated at, e.g., 400 K, with AIMD as a first step toward the situation in the liquid phase. Still, the cooperativity of the liquid phase in which each ion interacts with several others cannot be captured by an isolated ion pair. Hence, the influence of neighbors can be studied by comparing the spectra of the liquid phase and of an isolated ion pair.

Indeed, the spectra calculated for the three states mentioned above were rather different (see Figure 4a). Wavenumbers obtained for the ground-state structure of one ion pair differed at most from the two power spectra. In particular, around 3000 cm^{-1}, the wavenumbers were too high, even though the wavenumbers were not corrected by the factor 1.045; this might be due to the neglect of anharmonicity.[48] The power spectra of one ion pair in the gas phase at 400 K and 30 ion pairs in the liquid phase at 400 K were quite similar at high wavenumbers. But in the range of 500−1000 cm^{-1}, the signal structure was qualitatively different. At these wavenumbers, vibrations less localized than at high wavenumbers were observed and seemed to be more dependent on the ion's environment. As it can be seen in Figure 5, the spacial distribution of the anion around the cation was very different for the isolated ion pair from that of a liquid-like system. In the isolated ion pair, the anion was found mainly in the C^2H

dx.doi.org/10.1021/ct300152t | J. Chem. Theory Comput. 2012, 8, 1570−1579

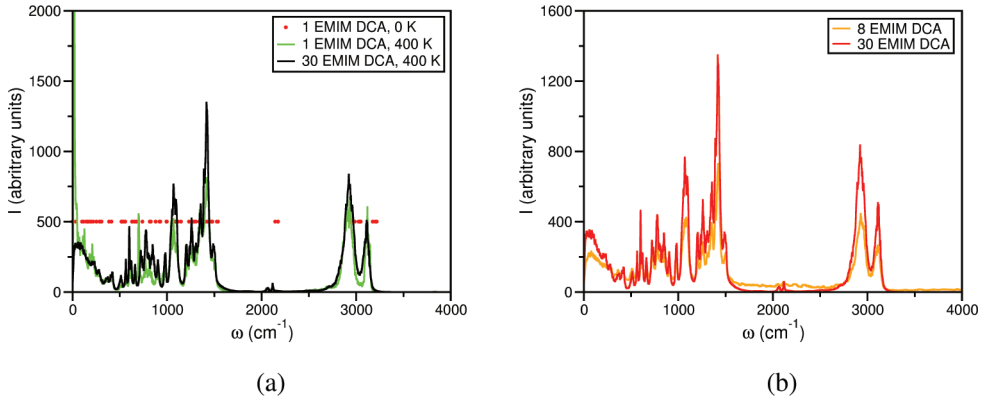

Figure 4. (a) Power spectra of an isolated EMIM DCA ion pair at 400 K and of 30 EMIM DCA ion pairs in liquid phase at 400 K as well as the (uncorrected) wavenumbers obtained for a ground-state configuration of one EMIM DCA ion pair and (b) power spectra of 8 and 30 EMIM DCA ion pairs in liquid phase at 400 K.

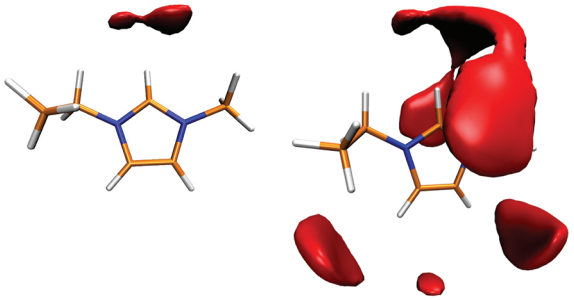

Figure 5. Isosurface of the spacial distribution function of the anion around the cation for (a) an isolated ion pair at an isovalue of 160 nm^{-3} and (b) 30 EMIM DCA ion pairs in liquid phase at an isovalue of 100 nm^{-3}.

hydrogen bond position. It is comprehensible that this had a significant impact on the vibrations in the fingerprint range.[83] Interestingly, the CH vibration signal at high wavenumbers was obtained for the isolated ion pair as in the liquid phase. The strong occupation of the C^2H hydrogen-bond position did not have significant influence. Hence, for the estimation of the hydrogen-bond strength, it may be sufficient to consider an isolated ion pair as the electronic effect seemed very local.

However, the maximum of intensity at around 60 cm^{-1} could not be found in the one ion pair's power spectrum, as the free rotation of the whole ion pair was possible. This rotation gave the most intense signal in the power spectrum of the isolated ion pair. For the bulk phase, the power spectra intensity approached 0 at 0 cm^{-1}. In this aspect, the power spectra of AIMD simulations of the liquid phase gave information not accessible by calculations of the other two states and in agreement with experimental spectra. Similar to the findings for the electrostatic properties, the power spectra of 8 ion pair simulations were almost identical to the power spectra of the 30 ion pair simulations (see Figure 4b). While the intensities of the signals varied slightly, the wavenumbers were the same. This strengthened the notion of locality over the short time dynamics, thus, the proposed ion cages hypothesis[19,23,52,84−90] is enforced. That might explain why the power spectra based on AIMD simulations were not system size dependent. The message obtained is the following: In order to reproduce spectra consistent with the experimental ones, it was necessary to describe the liquid environment. However, systems as small as eight ion pairs were sufficient and captured the short time dynamics. The influence of diffusion or ion cage dissociation is low at short times, as these occur on larger scales. In the short times characterized by the spectra, the ions rearrange and fluctuate mainly in the ion cages. Hence, the short time dynamics seemed associated to processes local in space. In the next section, we look in detail at one of these processes, namely the hydrogen bonding.

4.3. Hydrogen Bonding. Experimental IR spectra are widely used to evaluate the strength of hydrogen bonds.[21,31,33,35−37,39] Such a study is also possible with the power spectra based on AIMD simulations. As in experiments, the impact of hydrogen bonding was observed both at high wavenumbers around 3100 cm^{-1}[31,33,35,37] and at low wavenumbers below 200 cm^{-1}.[21,36]

As a first aspect, the aromatic CH bond-stretching vibrations showed a significant red shift for the ILs with stronger hydrogen bonds (see Figure 6a,c). This red shift is well-known as a characteristic of hydrogen bonding.[91] Qualitatively, the CH bond is weakened by the hydrogen bond as electron density from the hydrogen-bond acceptor atom is transferred into the antibonding CH σ^* orbital. In this way, the bond length of the CH bond increases, while the force constant and, thus, the wavenumber of the stretching vibration decrease. This red shift was obtained for the aromatic CH bond vibration in the range of 3060−3150 cm^{-1} but not for the aliphatic CH bond vibrations around 2800−3000 cm^{-1} (see Figure 6a). The assignment into aliphatic and aromatic CH bond vibrations became obvious if only the power spectra related to the single CH bonds were compared (see Figure 6b) and met the expectations.[92] This is an indication that the anions interacted mainly with the aromatic imidazolium ring hydrogens, as could be concluded also from the spacial distributions illustrated in Figure 5. In general, the similarity in the spectra of EMIM and BMIM ILs supported the finding that anions were distributed similarly around the cation and, thus, close to the imidazolium ring in all imidazolium-based ILs. In general, the signal of Cl-based ILs was the one with the largest red shift to lower wavenumbers pointing to the strongest hydrogen bonds (see Figure 6c). The signals of SCN based ILs were still slightly stronger red-shifted than the ones of DCA-based ILs. Thus, the shifts reflected the same order in hydrogen-bond strength as reported in literature.[26] Furthermore, the part power spectrum of the C^2H vibration depended only weakly on the side chain length (see Figure 6c). The difference between the C^2H bond

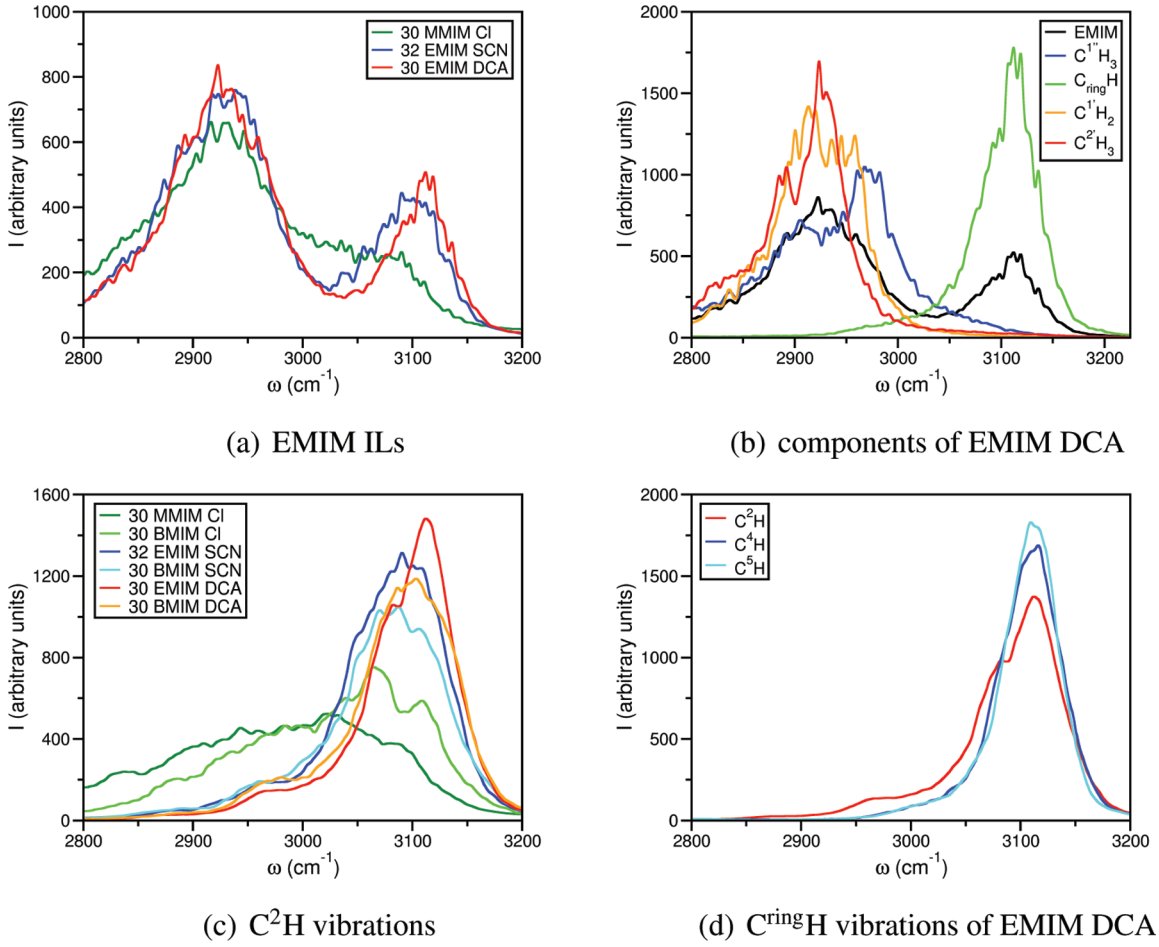

Figure 6. Power spectra at high wavenumbers between 2800 to 3200 cm^{-1}. In (a), the power spectra of MMIM Cl, EMIM SCN, and EMIM DCA are shown, in (b) the part power spectra of the different groups in EMIM DCA, in (c) the part power spectra of the C^2H bond for all studied ILs, and in (d) the part power spectra of the three ring CH bonds, C^2H, C^4H, and C^5H, for EMIM DCA (for nomenclature see Figure 1).

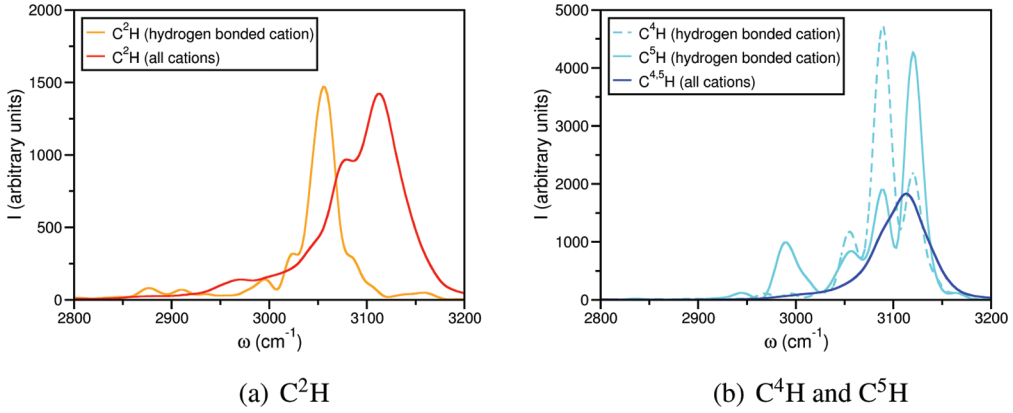

Figure 7. Part power spectra of (a) C^2H vibrations and (b) C^4H and C^5H vibrations of all cations and of a strongly hydrogen-bonded cation at high wavenumbers between 2800 and 3200 cm^{-1}.

power spectra of MMIM Cl and BMIM Cl might be due to the different DFT functionals used. As discussed for experimental IR spectra,[35,37] the C^2H vibration occurred at slightly lower wavenumbers than the C^4H or C^5H vibrations (see Figure 6d). This effect was also observed in the first and so far only other AIMD-based power spectrum on an IL[20] which suffered from rather limited statistics.

The power spectrum corresponding to the C^2H bond seemed to consist of two contributions, as there were two maxima at 3080 and 3110 cm^{-1} (see Figure 6d). Two contributions were also found by the deconvolution of an experimental spectrum.[37] The lower wavenumber contribution was attributed to ions which took part only in one hydrogen bond and, thus, were strongly polarized forming one strong hydrogen bond. The higher wavenumber contribution was proposed to be associated with ions incorporated in hydrogen-bonded networks. Corresponding two contributions were proposed for the C^4H or C^5H vibrations, too.[37] In contrast

dx.doi.org/10.1021/ct300152t | J. Chem. Theory Comput. 2012, 8, 1570−1579

here, the C^4H or C^5H bond spectra showed only one broad signal (see Figure 6d). Whereas the deconvolution of experimental spectra is always connected to a certain arbitrariness in the collection of fit functions, the power spectra of this work are obtained directly from the dynamics of the system; this, indeed, is an advantage if the signals shall be properly interpreted. The power spectra of the C^2H, C^4H, and C^5H bonds (see Figure 6d) suggest that all three bonds are similarly influenced by hydrogen bonds in most situations. However, only the C^2H bond seemed to form stronger hydrogen bonds in some situations. To further study this aspect, an ion pair forming a strong hydrogen bond via the C^2H hydrogen was picked out from the whole simulation data, and the power spectrum of only this ion pair was calculated. The corresponding power spectra of the C^2H, C^4H, and C^5H bonds are shown in Figure 7. Clearly, the C^2H bond vibration was significantly red-shifted as was expected for a strong hydrogen bond (see Figure 7a). The red shift was larger than that of the second maxima of the C^2H bond spectrum of all ion pairs. This implied that the C^2H bond vibration could adapt a whole range of wavenumbers depending significantly on the environment in the liquid phase. The description in terms of two discrete contributions as proposed[37] might have missed this decisive aspect. The C^4H and C^5H bond spectra did not exhibit a shift compared to the spectra obtained for all ion pairs (see Figure 7b). Still, the C^4H bond vibration had a lower wavenumber than that of the C^5H bond. Indeed, the C^4H hydrogen atom was closer to other anions than the C^5H one, as the C^5H hydrogen atom was more shielded by the ethyl side chain. In this way, the C^4H bond was more influenced by hydrogen bonds than the other. Hence also for these bonds, the environment seemed to have an impact on the vibration's wavenumber, even though the variation was lower than for the C^2H bond. This example of the power spectrum of one very strong hydrogen-bonded ion pair demonstrates how simulation-based spectra can help to interpret experimental spectra.

As a second aspect, at low wavenumbers, intermolecular vibrations, having small force constants, can be detected, and the wavenumber of the intensity maximum in the range of 50–200 cm^{-1} was proposed to correlate with the hydrogen-bond strength.[21,36] Experimentally, the intensity maximum was at 117.6 cm^{-1} for EMIM SCN and 113.5 cm^{-1} for EMIM DCA.[21] As shown in Figure 8, the intensity was rather constant at broad

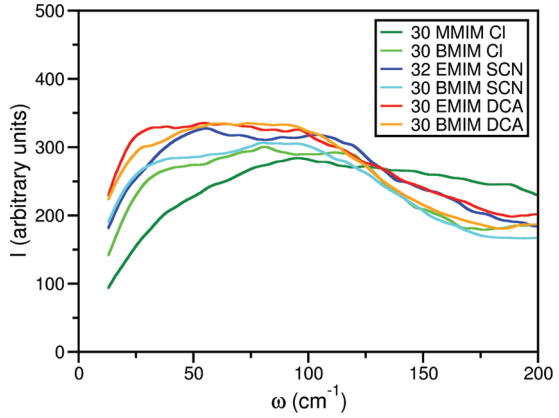

Figure 8. Smoothed power spectra in the range from 0 to 200 cm^{-1} of all studied ILs. The shown data points are averaged over 50 original data points.

maxima and, thus, the assignment of a wavenumber was ambiguous. But, the order could be characterized as follows: for MMIM Cl around 100 cm^{-1}, for EMIM SCN about 80 cm^{-1}, and for EMIM DCA 60 cm^{-1}. For the ILs with short side chains, the experimental trend was reproduced. Thus, a correlation to the hydrogen-bond strengths or at least some cation anion interaction[64] seemed to be confirmed. Still, the maxima occurred at different wavenumbers than in experiment. This might be due to the uncertainty of the wavenumbers and the assignment of the maximum or due to the different selection rules. In IR, terahertz, or Raman spectra, only certain vibrations are detected, what might lead to a different shape of the signal, as the single vibrations have changed intensities, and thus, the superposition is altered, too. Hence, the maximum of this broad absorption might be shifted. Although, the simulation times were mostly in the range of 10–20 ps. Thus, the statistics at low wavenumbers was poor, and the uncertainty of the power spectra intensities was high because a vibration with a wavenumber of 65 cm^{-1}, for instance, has a periodic time of 0.5 ps. For BMIM ILs, the differences between the intensity maxima were lower: BMIM Cl, 90 cm^{-1}; BMIM SCN, 80 cm^{-1}; and BMIM DCA, 70 cm^{-1}. As the maxima were very broad, there was no significant shift. Unfortunately, no experimental data for the BMIM ILs in this wavenumber range have been published so far. Thus, it is not possible to judge if these differences between ILs with short and long side chains are consistent with experiments. All groups of the ions, including the complete cation side chains, contributed to the low wavenumbers signal in the power spectra, and the influence of hydrogen bonding might be overlaid in the power spectra.

The influence of hydrogen bonding found in experiments was also visible in the AIMD-based power spectra and the AIMD simulations allowed to gain a more detailed molecular insight. For instance, it appeared unlikely that there were two distinct environments for the ions as proposed based on deconvolution of experimental spectra.[37] It seems that the strength of hydrogen bonds varied continuously, and thus, the CH bond vibrations can occur in a whole range of wavenumbers depending sensitively on the ions' environment. While hydrogen bonds change the molecular electronic structure, other, steric interactions lead to some preferred conformations of the ions. In the next section, the applicability of AIMD-based power spectra to study the internal conformational degrees of freedom is discussed.

4.4. Vibrations of the Cation. As expected for ILs with cations of different side chain length, the signal structure in the fingerprint range was found to be characteristic for each imidazolium cation and to depend on the side chain length. In the range of 300–1500 cm^{-1}, there were several signals which were detected for either EMIM or BMIM ILs (see Figure 2). The example with the highest intensity was found at about 775 cm^{-1} only for EMIM ILs (see Figure 9a). In fact, only the ethyl groups contributed to this, as can be seen from the part power spectra of the different groups of the EMIM (see Figure 9b). At around 730 cm^{-1}, both EMIM and BMIM ILs gave a signal (see Figure 9a) also found in experiments.[33,34,38] For EMIM DCA, this signal was purely connected to some imidazolium ring vibrations (see Figure 9b). For BMIM DCA, there were also contributions of the butyl chain at this wavenumber range (see Figure 9c). Hence, the similarity of the signals in the power spectra did not necessarily imply that they had the same origin. For BMIM-based ILs, the signal at around 730 cm^{-1} and a signal at 625 cm^{-1} were proposed to be associated with the

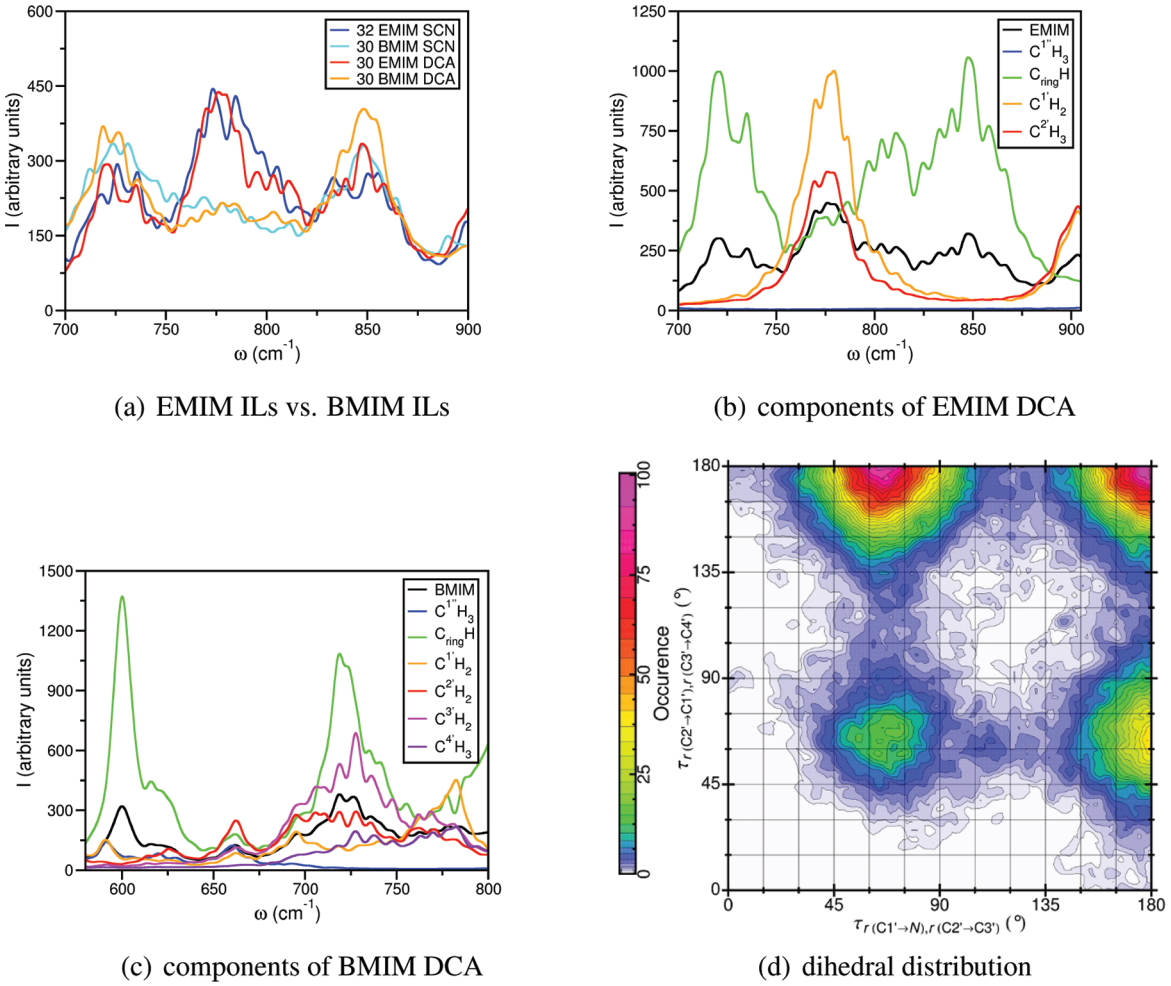

Figure 9. Power spectra in the range from 700 to 900 cm^{-1} of (a) EMIM SCN, BMIM SCN, EMIM DCA, and BMIM DCA, (b) part power spectra of different groups in EMIM DCA, and (c) part power spectra of different groups in BMIM DCA in the range between 650 and 800 cm^{-1}. In (d), the projection of the normalized probability distribution of finding the butyl side chain of the imidazolium cation with the dihedral angles $\tau_{r(C1'\rightarrow N),r(C2'\rightarrow C3')}$ and $\tau_{r(C2'\rightarrow C1'),r(C3'\rightarrow C4')}$ (for nomenclature see Figure 1). The probability was normalized such that the highest probability value is equal to 100 and the color scheme ranges from white (low) to violet (high).

anti−anti conformation of the butyl side chain.[33,45] The gauche−anti conformation of the butyl side chain, often found in ground-state structures,[43,45] was reported to be associated with signals at 600 and 700 cm^{-1}.[33,45,93] Whereas all BMIM ILs power spectra had bands at 730 and 600 cm^{-1}, there were no distinct signals observed at 625 or 700 cm^{-1} (see Figures 2 and 9c). Also, the signal at 600 cm^{-1} seemed to be connected to a ring vibration rather than to contributions of the side chain (see Figure 9c). Thus, the characteristic signals found in ground-state structures of ion pairs[45] and experimental Raman spectra of crystals[93] could not be reproduced here. The combined probability distribution for the decisive dihedrals suggested that the gauche−anti and anti−anti arrangements of the butyl side chain were similarly likely for BMIM DCA (see Figure 9d). There was a lower probability for anti−gauche or gauche−gauche conformations, which was expected due to steric effects.

5. CONCLUSION

Power spectra were calculated based on AIMD simulations for several ILs. They were found to be consistent in wavenumbers, but not intensities, both with experimental IR or Raman spectra and with respect to each other. The consistency between theory and experiment was observed only if liquid-like systems were considered. Vibration frequencies based on ground-state structures and also the power spectrum of an isolated ion pair at 400 K were found to be inconsistent with experiments. They neglected molecular cooperativity and did not describe the many-molecule configurational space properly. However, power spectra based on an AIMD simulation of only 8 ion pairs described the same signal structure as the one of a 30 ion pair simulation. This strengthened the suggestion of locality discussed in previous works.[46,47,55] Short simulation times of about 10 ps seemed sufficient to give consistent power spectra, and this suggested locality of the short time dynamics in time, too. The observed locality in space and time is consistent with the proposed ion cage dynamics,[19,23,52,84−90] meaning that the ions cannot diffuse much on the short time scale but stay in their ion cages. Hence, AIMD studies of small systems representing a liquid sample were sufficiently accurate for understanding molecular mechanisms in the liquid phase and can be used for modeling purposes, e.g., classical force field design.

In general, the power spectra provided useful analyses of the molecular processes in the liquid environment. They reproduced the experimental trend in hydrogen-bond strength

and allowed for its detailed interpretation. By selecting specific bonds or ions, it was possible to shed light onto the origin of the signal shape of the aromatic CH bond vibration. The CH bond vibration was found to be very sensitive to the liquid environment. As a consequence, the hypothesis of two distinct environments[37] seemed not sufficient to describe the continuous shift of the vibration's wavenumber. Finally, signals associated with the side chain conformations of the imidazolium cations were detected and found to be characteristic for the cation.

In this respect, the power spectra can be used as a tool of validation of the approach used, and at the same time, they provide important information for interpreting the experimental data and for modeling ILs at molecular level.

■ ASSOCIATED CONTENT

Supporting Information

This material is available free of charge via the Internet at http://pubs.acs.org.

■ AUTHOR INFORMATION

Corresponding Author

*E-mail: luigi.dellesite@fu-berlin.de.

Notes

The authors declare no competing financial interest.

■ ACKNOWLEDGMENTS

Florian Dommert is acknowlegded for providing the equilibrated start configurations for the AIMD simulations. All authors would like to thank the DFG priority program 1191 "Ionic Liquids" for funding, Denis Andrienko for critical reading of the manuscript, and the RZG of the Max Planck Society for providing the necessary computer time.

■ REFERENCES

(1) Rogers, R. D.; Seddon, K. R. *Science* **2003**, *302*, 792−793.
(2) *Ionic Liquids in Synthesis*; Wasserscheid, P., Welton, T., Eds.; Wiley-VCH: Weinheim, Germany2007.
(3) Plechkova, N. V.; Seddon, K. R. *Chem. Soc. Rev.* **2008**, *37*, 123−150.
(4) Armand, M.; Endres, F.; MacFarlane, D. R.; Ohno, H.; Scrosati, B. *Nat. Mater.* **2009**, *8*, 621−629.
(5) Pinkert, A.; Marsh, K. N.; Pang, S.; Staiger, M. P. *Chem. Rev.* **2009**, *109*, 6712−6728.
(6) Castner, E. W.; Wishart, J. F. *J. Chem. Phys.* **2010**, *132*, 120901.
(7) Giernoth, R. *Angew. Chem., Int. Ed.* **2010**, *49*, 2834−2839.
(8) Liu, H.; Liu, Y.; Li, J. *Phys. Chem. Chem. Phys.* **2010**, *12*, 1685−1697.
(9) Olivier-Bourbigou, H.; Magna, L.; Morvan, D. *Appl. Catal., A* **2010**, *373*, 1−56.
(10) Werner, S.; Haumann, M.; Wasserscheid, P. *Annu. Rev. Chem. Biomol. Eng.* **2010**, *1*, 203−230.
(11) Kirchner, B. *Top. Curr. Chem.* **2009**, *290*, 213−262.
(12) Ballone, P.; Pinilla, C.; Kohanoff, J.; Del Pópolo, M. G. *J. Phys. Chem. B* **2007**, *111*, 4938−4950.
(13) Spohr, H. V.; Patey, G. N. *J. Chem. Phys.* **2009**, *130*, 104506.
(14) Spohr, H. V.; Patey, G. N. *J. Chem. Phys.* **2010**, *132*, 154504.
(15) Spohr, H. V.; Patey, G. N. *J. Chem. Phys.* **2010**, *132*, 234510.
(16) Zahn, S.; Bruns, G.; Thar, J.; Kirchner, B. *Phys. Chem. Chem. Phys.* **2008**, *10*, 6921−6924.
(17) Zahn, S.; Uhlig, F.; Thar, J.; Spickermann, C.; Kirchner, B. *Angew. Chem., Int. Ed.* **2008**, *47*, 3639−3641.
(18) Lehmann, S. B. C.; Roatsch, M.; Schöppke, M.; Kirchner, B. *Phys. Chem. Chem. Phys.* **2010**, *12*, 7473−7486.
(19) Zahn, S.; Thar, J.; Kirchner, B. *J. Chem. Phys.* **2010**, *132*, 124506.
(20) Bhargava, B.; Balasubramanian, S. *Chem. Phys. Lett.* **2006**, *417*, 486−491.
(21) Fumino, K.; Wulf, A.; Ludwig, R. *Angew. Chem., Int. Ed.* **2008**, *47*, 3830−3834.
(22) Qiao, B.; Krekeler, C.; Berger, R.; Delle Site, L.; Holm, C. *J. Phys. Chem. B* **2008**, *112*, 1743−1751.
(23) Thar, J.; Brehm, M.; Seitsonen, A. P.; Kirchner, B. *J. Phys. Chem. B* **2009**, *113*, 15129−15132.
(24) Dommert, F.; Schmidt, J.; Krekeler, C.; Zhao, Y. Y.; Berger, R.; Delle Site, L.; Holm, C. *J. Mol. Liq.* **2010**, *152*, 2−8.
(25) Costa Gomes, M. F.; Canongia Lopes, J. N.; Pádua, A. *Top. Curr. Chem.* **2009**, *290*, 161−183.
(26) Stark, A. *Top. Curr. Chem.* **2009**, *290*, 41−81.
(27) Roth, C.; Peppel, T.; Fumino, K.; Köckerling, M.; Ludwig, R. *Angew. Chem., Int. Ed.* **2010**, *49*, 10221−10224.
(28) Peppel, T.; Roth, C.; Fumino, K.; Paschek, D.; Köckerling, M.; Ludwig, R. *Angew. Chem., Int. Ed.* **2011**, *50*, 6661−6665.
(29) Bernard, U. L.; Izgorodina, E. I.; MacFarlane, D. R. *J. Phys. Chem. C* **2010**, *114*, 20472−20478.
(30) Tait, S.; Osteryoung, R. A. *Inorg. Chem.* **1984**, *23*, 4352−4360.
(31) Suarez, P.; Einloft, S.; Dullius, J.; de Souza, R.; Dupont, J. *J. Chim. Phys. Phys.-Chim. Biol.* **1998**, *95*, 14−14.
(32) Paulechka, Y. U.; Kabo, G. J.; Blokhin, A. V.; Vydrov, O. A.; Magee, J. W.; Frenkel, M. *J. Chem. Eng. Data* **2003**, *48*, 457−462.
(33) Chang, H.-C.; Jiang, J.-C.; Su, J.-C.; Chang, C.-Y.; Lin, S. H. *J. Phys. Chem. A* **2007**, *111*, 9201−9206.
(34) Fujii, K.; Seki, S.; Fukuda, S.; Kanzaki, R.; Takamuku, T.; Umebayashi, Y.; Ishiguro, S.-i. *J. Phys. Chem. B* **2007**, *111*, 12829−12833.
(35) Fumino, K.; Wulf, A.; Ludwig, R. *Angew. Chem., Int. Ed.* **2008**, *47*, 8731−8734.
(36) Wulf, A.; Fumino, K.; Ludwig, R. *Angew. Chem., Int. Ed.* **2010**, *49*, 449−453.
(37) Köddermann, T.; Wertz, C.; Heintz, A.; Ludwig, R. *ChemPhysChem* **2006**, *7*, 1944−1949.
(38) Kiefer, J.; Fries, J.; Leipertz, A. *Appl. Spectrosc.* **2007**, *61*, 1306−1311.
(39) Wulf, A.; Fumino, K.; Ludwig, R. *J. Phys. Chem. A* **2010**, *114*, 685−686.
(40) Lassègues, J. C.; Grondin, J.; Holomb, R.; Johansson, P. *J. Raman Spectrosc.* **2007**, *38*, 551−558.
(41) Köddermann, T.; Fumino, K.; Ludwig, R.; Canongia Lopes, J. N.; Pádua, A. A. H. *ChemPhysChem* **2009**, *10*, 1181−1186.
(42) Dommert, F.; Holm, C. unpublished work, 2009−2011.
(43) Hunt, P. A.; Gould, I. R. *J. Phys. Chem. A* **2006**, *110*, 2269−2282.
(44) Dhumal, N. R. *Chem. Phys.* **2007**, *342*, 245−252.
(45) Hunt, P. A. *J. Phys. Chem. B* **2007**, *111*, 4844−4853.
(46) Wendler, K.; Zahn, S.; Dommert, F.; Berger, R.; Holm, C.; Kirchner, B.; Delle Site, L. *J. Chem. Theory Comput.* **2011**, *7*, 3040−3044.
(47) Wendler, K.; Dommert, F.; Zhao, Y. Y.; Berger, R.; Holm, C.; Delle Site, L. *Faraday Discuss.* **2012**, *154*, 111−132.
(48) Kuo, I.-F. W.; Tobias, D. J. *J. Phys. Chem. A* **2002**, *106*, 10969−10976.
(49) Tangney, P.; Scandolo, S. *J. Chem. Phys.* **2002**, *116*, 14−24.
(50) Iftimie, R.; Tuckerman, M. E. *J. Chem. Phys.* **2005**, *122*, 214508−214508.
(51) Gaigeot, M. P.; Vuilleumier, R.; Sprik, M.; Borgis, D. *J. Chem. Theory Comput.* **2005**, *1*, 772−789.
(52) Buhl, M.; Chaumont, A.; Schurhammer, R.; Wipff, G. *J. Phys. Chem. B* **2005**, *109*, 18591−18599.
(53) Del Pópolo, M. G.; Lynden-Bell, R. M.; Kohanoff, J. *J. Phys. Chem. B* **2005**, *109*, 5895−5902.
(54) Prado, C. E. R.; Del Pópolo, M. G.; Youngs, T. G. A.; Kohanoff, J.; Lynden-Bell, R. M. *Mol. Phys.* **2006**, *104*, 2477−2483.
(55) Krekeler, C.; Dommert, F.; Schmidt, J.; Zhao, Y. Y.; Holm, C.; Berger, R.; Delle Site, L. *Phys. Chem. Chem. Phys.* **2010**, *12*, 1817−1821.

(56) Bagno, A.; D'Amico, F.; Saielli, G. *ChemPhysChem* **2007**, *8*, 873−881.
(57) Bhargava, B. L.; Balasubramanian, S. *J. Phys. Chem. B* **2007**, *111*, 4477−4487.
(58) Ghatee, M. H.; Ansari, Y. *J. Chem. Phys.* **2007**, *126*, 154502.
(59) Spickermann, C.; Thar, J.; Lehmann, S. B. C.; Zahn, S.; Hunger, J.; Buchner, R.; Hunt, P. A.; Welton, T.; Kirchner, B. *J. Chem. Phys.* **2008**, *129*, 104505.
(60) Zahn, S.; Wendler, K.; Delle Site, L.; Kirchner, B. *Phys. Chem. Chem. Phys.* **2011**, *13*, 15083−15093.
(61) Kirchner, B.; Seitsonen, A. P. *Inorg. Chem.* **2007**, *46*, 2751−2754.
(62) Mallik, B. S.; Siepmann, J. I. *J. Phys. Chem. B* **2010**, *114*, 12577−12584.
(63) Bhargava, B. L.; Balasubramanian, S. *J. Phys. Chem. B* **2008**, *112*, 7566−7573.
(64) Sarangi, S. S.; Reddy, S. K.; Balasubramanian, S. *J. Phys. Chem. B* **2011**, *115*, 1874−1880.
(65) Frenkel, D.; Smit, B. *Understanding Molecular Simulation*; 2nd ed.: From Algorithms to Applications; Academic Press: San Diego, CA, 2001.
(66) Wiener, N. *Acta Math.* **1930**, *55*, 117−258.
(67) Khinchin, A. *Math. Ann.* **1934**, *109*, 604−615.
(68) Butz, T. *Fourier Transformation for Pedestrians*; Springer: Berlin, Heidelberg, Germany, 2005.
(69) Brehm, M.; Kirchner, B. *J. Chem. Inf. Model.* **2011**, *51*, 2007−2023.
(70) Sprik, M.; Hutter, J.; Parrinello, M. *J. Chem. Phys.* **1996**, *105*, 1142−1142.
(71) Car, R.; Parrinello, M. *Phys. Rev. Lett.* **1985**, *55*, 2471.
(72) *CPMD*; IBM and Max-Planck Institut, Stuttgart: Armonk, New York and Stuttgart, Germany, 1997−2001; http://www.cpmd.org/.
(73) Nosé, S. *J. Chem. Phys.* **1984**, *81*, 511.
(74) Hoover, W. G. *Phys. Rev. A* **1985**, *31*, 1695−1695.
(75) Becke, A. D. *Phys. Rev. A* **1988**, *38*, 3098−3098.
(76) Lee, C.; Yang, W.; Parr, R. G. *Phys. Rev. B* **1988**, *37*, 785−789.
(77) Grimme, S. *J. Comput. Chem.* **2006**, *27*, 1787−1799.
(78) Zahn, S.; Kirchner, B. *J. Phys. Chem. A* **2008**, *112*, 8430−8435.
(79) Izgorodina, E. I.; Bernard, U. L.; MacFarlane, D. R. *J. Phys. Chem. A* **2009**, *113*, 7064−7072.
(80) Koel, M. *Proc. Estonian Acad. Sci. Chem.* **2000**, *49*, 145−155.
(81) Bortnuchik, A. L.; Stepukhovich, A. D.; Rabinovich, I. S. *J. Appl. Spectrosc.* **1973**, *19*, 923−925.
(82) Lessing, J. G. V.; Fouché, K. F.; Retief, T. T. *J. Chem. Soc., Dalton Trans.* **1977**, 2024−2029.
(83) Malberg, F.; Pensado, A. S.; Kirchner, B. submitted 2012.
(84) Morrow, T. I.; Maginn, E. J. *J. Phys. Chem. B* **2002**, *106*, 12807−12813.
(85) Del Pópolo, M. G.; Voth, G. A. *J. Phys. Chem. B* **2004**, *108*, 1744−1752.
(86) Yan, T.; Burnham, C. J.; Del Pópolo, M. G.; Voth, G. A. *J. Phys. Chem. B* **2004**, *108*, 11877−11881.
(87) Bhargava, B. L.; Balasubramanian, S. *J. Chem. Phys.* **2005**, *123*, 144505.
(88) Turton, D. A.; Hunger, J.; Stoppa, A.; Hefter, G.; Thoman, A.; Walther, M.; Buchner, R.; Wynne, K. *J. Am. Chem. Soc.* **2009**, *131*, 11140−11146.
(89) Méndez-Morales, T.; Carrete, J.; Cabeza, O.; Gallego, L. J.; Varela, L. M. *J. Phys. Chem. B* **2011**, *115*, 6995−7008.
(90) Kohagen, M.; Brehm, M.; Thar, J.; Zhao, W.; Müller-Plathe, F.; Kirchner, B. *J. Phys. Chem. B* **2011**, *115*, 693−702.
(91) Steiner, T. *Angew. Chem., Int. Ed.* **2002**, *41*, 48−76.
(92) Hesse, M.; Meier, H.; Zeeh, B. *Spektroskopische Methoden in der organischen Chemie*; Thieme: Stuttgart, Germany, 2005.
(93) Hayashi, S.; Ozawa, R.; Hamaguchi, H.-o. *Chem. Lett.* **2003**, *32*, 498−499.